

## Mixing and Viscosity Determinations with Helical Ribbon Impeller

L. Slemenik Perše and M. Žumer

University of Ljubljana, Faculty of Chemistry and Chemical Technology,  
Aškerčeva 5, SI-1000 Ljubljana, Slovenia  
E-mail: lidija.slemenik@uni-lj.si

Original scientific paper  
Received: December 3, 2003  
Accepted: May 24, 2004

Fluids with complex rheological properties often exhibit shear dependence and/or time dependence. Due to high viscosity and complex rheological behavior, mixing of such fluids is usually performed in the laminar flow regime.

The object of this work was to study the mixing of highly viscous and rheologically complex fluids with single-flight helical ribbon impeller. Highly viscous motor oils were used as Newtonian fluids, while two different types of non-Newtonian fluids were used. Carboxymethyl cellulose represented well-known shear thinning non-Newtonian fluid, and welan solutions represented rheologically complex and more structured non-Newtonian fluid. Torque was measured at different impeller speeds in order to obtain power curves and to calculate viscosity of different non-Newtonian fluids as a function of impeller speed.

The results of the mixing study of different highly viscous fluids showed that the torque depended on the impeller speed and the rheological properties of the fluid. Shear rate constant  $K_s$  was determined for non-Newtonian fluids with different rheological properties and it was shown that  $K_s$  depends on fluids properties. The comparison between mixing experiments and rheological measurements showed that the shear-dependent viscosity could be determined during the mixing process by measuring the torque on the impeller.

*Key words:*

Mixing, rheology, carboxymethyl cellulose, welan, helical ribbon impeller

### Introduction

The fluid viscosity or more precisely the shear dependence of the viscosity, is often considered as the most important rheological function. With respect to mixing, fluids are usually classified in two categories: the low-viscosity fluids and the high-viscosity fluids. The rheological behavior of high-viscosity fluids is in general complex and may include shear-dependent, viscoelastic and time-dependent properties. Mixing of such fluids is therefore complicated and requires special consideration. Particularly important is the use of a proper mixing equipment, which in general consists of a mixing vessel, an impeller and a motor. Impellers with small ratio between the diameter of the impeller and the diameter of the vessel are quite inefficient, since the high apparent viscosity of the fluid creates stagnant zones in the fields of low shear, far from the impeller. In order to eliminate these regions and to obtain effective mixing of the entire tank contents, close-clearance impellers with large ratio of the impeller diameter to the diameter of the vessel are commonly used. Many authors<sup>1-5</sup> have studied mixing of complex fluids with different close-clearance impellers and they have shown that helical ribbon impellers are very efficient as they provide shorter

mixing times and thus require less energy to reach a specified level of homogeneity.

For describing and especially for properly designing a mixing process, macroscopic quantities like flow patterns, power consumption, and mixing and circulation times, are usually used. Power consumption is the energy transferred from the impeller to the fluid per unit time. It is closely related to the costs of mixing process and represents important design parameter in many industrial applications. Power consumption depends on the fluid and it is strongly affected by the flow pattern.

Power characteristics of impeller system are commonly expressed by a power curve – dimensionless Reynolds number,  $Re$ , vs. dimensionless power number,  $P_0$ . In stirred tanks, the Reynolds number is defined as:

$$Re = \frac{\rho N d^2}{\eta} \quad (1)$$

where  $N$  is the impeller speed,  $d$  is the diameter of the impeller, and  $\rho$  and  $\eta$  are the fluid density and dynamic viscosity, respectively. The value of the Reynolds number characterizes the type of the flow regime. It is known that the flow is fully turbulent

at high Reynolds numbers, typically  $Re > 10^4$ , while laminar flow regime is usually restricted to low Reynolds numbers,  $Re < 10$ .

The dimensionless power number is defined as

$$P_0 = \frac{P}{\rho N d^5} \quad (2)$$

where  $P$  is power input, which is a function of operating conditions, fluid properties and the geometry of the mixing vessel.<sup>6</sup> It can be calculated from the torque measurements:

$$P = 2 \pi N M. \quad (3)$$

In the region of laminar flow ( $Re < 10$ ) the power number,  $P_0$ , is inversely proportional to the Reynolds number:

$$P_0 = C Re^{-1}, \quad (4)$$

where  $C$  is a constant that depends on mixing system. Combining equations (1) to (4), one can obtain the viscosity of the fluid:

$$\eta = \frac{2\pi M}{C N d^3} \quad (5)$$

which is possible to determine only, when the constant  $C$  is known. Constant  $C$  can be determined by a set of experimental data (torque at different impeller speeds) obtained by mixing a Newtonian fluid of known density and viscosity in the laminar flow regime. If the obtained data are plotted in the form of power number,  $P_0$ , vs. Reynolds number,  $Re$ , (equation (4)), the constant  $C$  can be directly evaluated from the curve. In this manner, the viscosity as a function of impeller speed can be determined during the mixing process by measuring the torque induced on the impeller. This is especially important for suspensions, fermentation broths and other non-homogeneous fluids. For such fluids, the viscosity measurements obtained by using conventional rheometers are of rather limited value, because of gravity settling of the suspended particles, and/or other forms of phase separation.<sup>7</sup>

By definition, the viscosity,  $\eta$ , is equal to the ratio of shear stress,  $\tau$ , to shear rate,  $\dot{\gamma}$ :<sup>8</sup>

$$\eta = \frac{\tau}{\dot{\gamma}}. \quad (6)$$

For the average shear rate around the impeller, Metzner and Otto<sup>9</sup> proposed the relation:

$$\dot{\gamma} = K_s N \quad (7)$$

where the constant  $K_s$  depends on the mixing system.

The rheological properties of shear-thinning fluids can be expressed by power law:

$$\tau = k \dot{\gamma}^n \quad (8)$$

and

$$\eta = k \dot{\gamma}^{n-1} \quad (9)$$

where  $k$  and  $n$  are consistency index and flow behavior index, respectively. Combining equations (6) to (9), the viscosity is given:

$$\eta = k(K_s N)^{n-1}. \quad (10)$$

Comparing equations (5) and (10) one obtains:

$$\frac{2\pi M}{C N d^3} = k(K_s N)^{n-1} \quad (11)$$

From the above relation (equation (11)) the constant  $K_s$  can be determined by obtaining a set of experimental data in laminar flow regime using a non-Newtonian fluid of known rheological properties.

The paper reports on an experimental mixing study of Newtonian and non-Newtonian fluids in a stirred tank with a single-flight helical ribbon impeller. Two Newtonian motor oils with different viscosities and non-Newtonian CMC and welan solutions of different concentrations, were used. The results presented include torque as a function of impeller speed, power curve, and viscosity as a function of shear rate around impeller. A comparison between the shear dependence of viscosity obtained by rheological measurements and viscosity determined during mixing experiments, is reported. The calculation of  $K_s$  from the correlation from literature is also compared with the calculated  $K_s$  from experimental data.

## Experimental

### Equipment

A mixing system of our own design (Fig. 1) was used to conduct experiments for mixing highly viscous fluids. The measuring system consisted of a motor, a torque transducer and a flat-bottomed plexiglass vessel, equipped with single-flight helical ribbon impeller. The impeller was rotated by means of a 2.2 kW motor (Unidrive UNI 1404, Control Techniques) with variable speed control (from 0 to 200 rpm). The torque was measured using a torque transducer (T20WN/2NM, HBM) with an operating range of 0–2 N m. The torque, measured with only air in the mixing vessel, was zero,

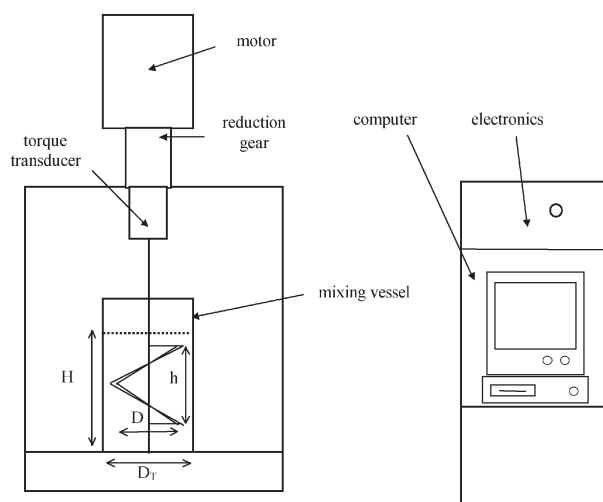


Fig. 1 – Experimental mixing system with helical ribbon impeller (diameter of the vessel,  $D_T = 0.185$  m, height of the fluid,  $H = 0.22$  m, diameter of the impeller,  $D = 0.16$  m, the ribbon width,  $W = 0.03$  m, height of the impeller  $h = 0.16$  m)

which indicates that torque due to the bearings, couplings and so forth, was insignificant.

The mechanical part of the mixing system was connected to the computer, which enabled the control of the process and acquisition of the experimental data. For measuring the temperature a temperature sensor Pt100 was inserted in the fluid through the vessel wall. Another temperature sensor was placed outside the vessel in order to follow the temperature changes in the surroundings. The outputs from the sensors and the torque transducer were recorded in a computer as a function of time and impeller speed.

A rotational controlled stress rheometer (HAAKE RheoStress RS150), equipped with a cone-and-plate sensor system (C 60/4°), was used to examine the rheological properties of different fluids, used in the mixing study.

### Test fluids and methods

Two motor oils (BRT150 and Cylinder oil, both from OLMA, Ljubljana) with different viscosities were used as Newtonian fluids, while aqueous solutions of carboxymethyl cellulose (Blanose Cellulose Gum 7HF, obtained in powdered form from Hercules, Aqualon) and welan (Welan Gum K1C376, obtained in powdered form from Kelco) represented non-Newtonian fluids. Different mass fraction of CMC ( $w = 2\%$  and  $2.5\%$ ) and welan ( $w = 1\%$ ,  $1.5\%$  and  $2\%$ ) solutions were prepared by dissolving dry powdered polymer in distilled water at ambient temperature.

The rheological tests under steady shear conditions were carried out in the shear rate range  $1 \leq \dot{\gamma} \leq 100$  s<sup>-1</sup>. The rheological characterization

of non-Newtonian CMC and welan solutions was performed also under non-destructive conditions of oscillatory shear. To allow temperature variations during mixing experiments, the same rheological tests were carried out at different temperatures.

Mixing was studied by measuring the torque as a function of the impeller speed. During the experiments, the temperature of the fluid in the mixing vessel was in the range from 22 °C to 25 °C.

## Results and discussion

### Rheological characterisation

Both motor oils exhibited shear- and time-independent Newtonian flow behavior. The oils differed in values of viscosity and density (Table 1). The CMC and welan solutions exhibited non-Newtonian shear-thinning behavior. Under the conditions of steady shear, time dependent effects were not detected. In the shear rate range examined ( $1 \leq \dot{\gamma} \leq 100$  s<sup>-1</sup>), the shear thinning behavior was described by the power law relation (equation (8) and (9)) with the quantities  $k$  and  $n$  reported in Table 2.

Table 1 – Properties of Newtonian fluids at  $T = 25$  °C

	$\eta$ (Pa s)	$\rho$ (kg m <sup>-3</sup> )
brt150	1.5	895
co	3.8	905

Table 2 – Values of power-law indices for CMC and welan solutions at  $T = 25$  °C

	2 % wt. CMC	2.5 % wt. CMC	1 % wt. W	1.5 % wt. W	2 % wt. W
$k$ (Pa·s <sup>n</sup> )	18.66	36.19	26.01	54.58	84.35
$n$ (/)	0.4023	0.3638	0.0811	0.0635	0.0499

The rheological tests were performed at different temperatures from 20 °C to 30 °C. The viscosity of Newtonian fluids and CMC solutions decreased with increasing temperature. It was observed that the decrease of viscosity with temperature was more significant for motor oils ( $\sim 7\%$  °C<sup>-1</sup>) than for CMC solutions ( $\sim 2\%$  °C<sup>-1</sup> for  $w = 2\%$  CMC and  $\sim 3.5\%$  °C<sup>-1</sup> for  $w = 2.5\%$  CMC). The effect of temperature was negligible for all welan solutions (Fig. 2).

Due to non-Newtonian properties of CMC and welan solutions, the rheological properties of these

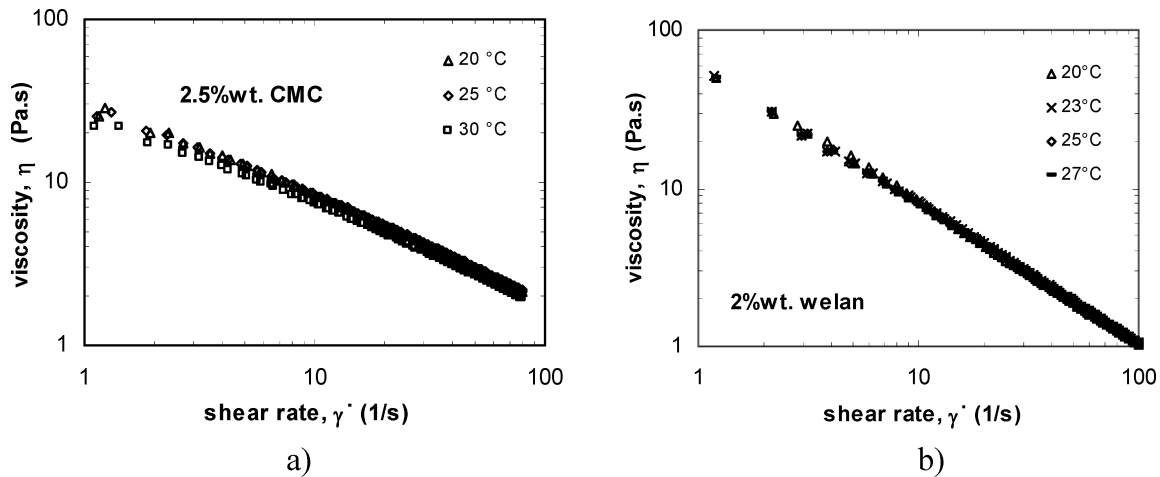


Fig. 2 – The effect of temperature on shear dependent viscosity for a) 2.5 % wt. CMC solution and b) 2 % wt. welan solution

solutions were examined also under non-destructive conditions of oscillatory shear. The results showed that non-Newtonian fluids exhibited elastic ( $G'$ ) and viscous ( $G''$ ) contribution to viscoelastic flow behavior.

The upper limit of linear viscoelastic region was determined from stress sweep tests at constant angular frequency of  $6.28 \text{ rad s}^{-1}$ . The extent of the linear region for both CMC solutions ranged up to 40 % of the deformation amplitude, while for welan solutions linear region was only up to 20 %. Frequency dependence for both dynamic moduli was examined at constant deformation amplitude (10 %) that enabled linear viscoelastic regime for all the fluids and throughout the whole frequency range examined. Similar frequency dependence of dynamic moduli was observed for both CMC solutions (Fig. 3a). In the low frequency range, the viscous contribution ( $G''$ ) prevailed over the elastic one, whereas at higher frequencies the elastic contribution ( $G'$ ) was predominant. The crossover point, at which both moduli had the same value,

depended on polymer concentration and it was for higher mass fraction of CMC ( $w = 2.5 \%$  CMC) shifted toward lower frequency. Such behavior can usually be found in concentrated polymer solutions.

Frequency dependency of welan solutions (Fig. 3b) differed from that for CMC solutions. For all the concentrations of welan elastic contribution ( $G'$ ) strongly prevailed over the viscous one ( $G''$ ) in the whole frequency range examined. Both dynamic moduli slightly increased with the increasing frequency, but the increase was less pronounced than for CMC solutions. Behavior like this is characteristic for weak gels.

### Mixing

Torque measurements at various impeller speeds were performed for Newtonian and non-Newtonian fluids. The results are shown in Fig. 4 and Fig. 5. As it was expected, the values of the torque were higher for the fluids with higher viscosity. For

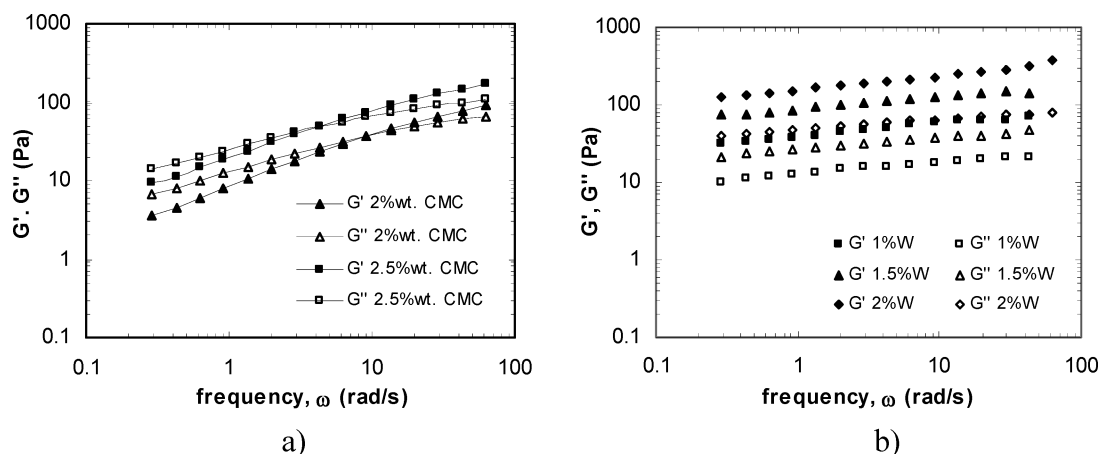


Fig. 3 – Frequency dependence of  $G'$  and  $G''$  for CMC solutions used for mixing at  $T = 25 \text{ }^\circ\text{C}$

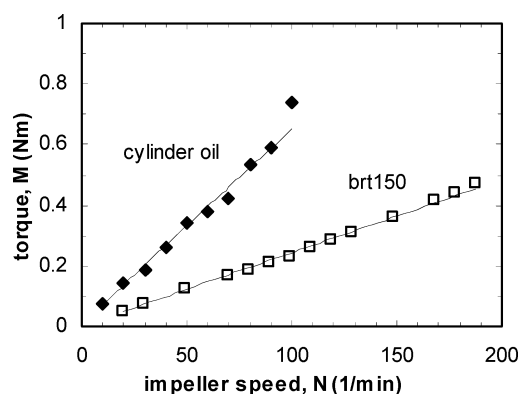


Fig. 4 – The dependence of torque,  $M$ , on impeller speed,  $N$ , for Newtonian oils

Newtonian oils the torque linearly increased with increasing impeller speed (Fig. 4), while for all non-Newtonian solutions (Fig. 5) the dependence was non-linear. However, due to different rheological properties of CMC and welan, the dependence of the torque on impeller speed was not the same. The increase of the torque with the impeller speed was more pronounced for CMC solutions, whereas for welan solutions the increase was smaller, especially at lower impeller speeds.

From measurements of torque at different impeller speed, power curves (the dependence of the power number,  $P_o$ , on the Reynolds number,  $Re$ ) were determined for all the fluids used. It can be seen from Fig. 6 that in the range of  $0.3 < Re < 40$  the power curves had the same slope of  $-1$ , which is characteristic of a laminar flow regime. The constant  $C$  was evaluated from equation (4) and had for Newtonian fluids and CMC solutions a value of 153. Due to complex rheological properties, especially more pronounced elastic properties, power curves for welan solutions were vertically shifted towards higher values of power number. Hence, the constants  $C$  for different concentrations of welan had values 410, 215 and 207, respectively.

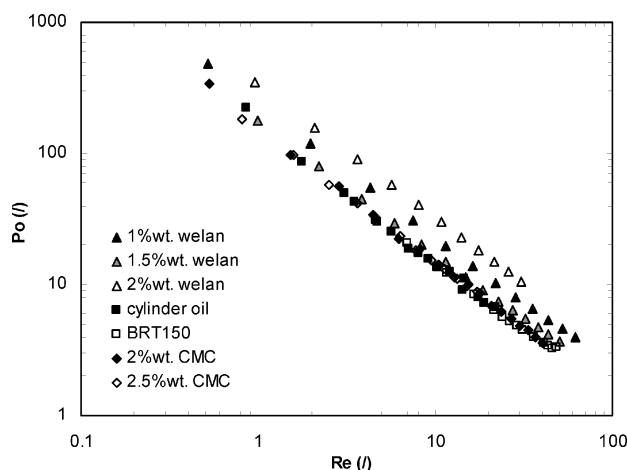


Fig. 6 – The “power curve” for a helical ribbon impeller - dependence of the dimensionless power number,  $P_o$ , on dimensionless Reynolds number,  $Re$ , for all fluids used

### Rheology – Mixing

In a rotational rheometer, the shear stress in the fluid,  $\tau$ , is deduced from a measurement of the torque,  $M$ , on the sensor system. The shear rate dependent shear stress, determined from rheological tests, was compared to the dependence of the torque (induced on the impeller in mixing vessel) on the impeller speed. The dependences of the torque,  $M$ , on impeller speed,  $N$ , and shear stress,  $\tau$ , on shear rate,  $\dot{\gamma}$ , are shown in Fig. 7. The results obtained by rheological measurements were comparable with the mixing results. The dependences of shear stress on shear rate and torque on impeller speed had the same slope, but the differences were observed in the magnitude of the values of shear stress and torque, respectively. In Fig. 7 the comparison between rheological measurements and mixing experiments are presented for  $w = 2.5\%$  CMC and  $w = 1.5\%$ , but the same was observed for all fluids used.

By rheological measurements, the viscosity as a function of shear rate was determined from equa-

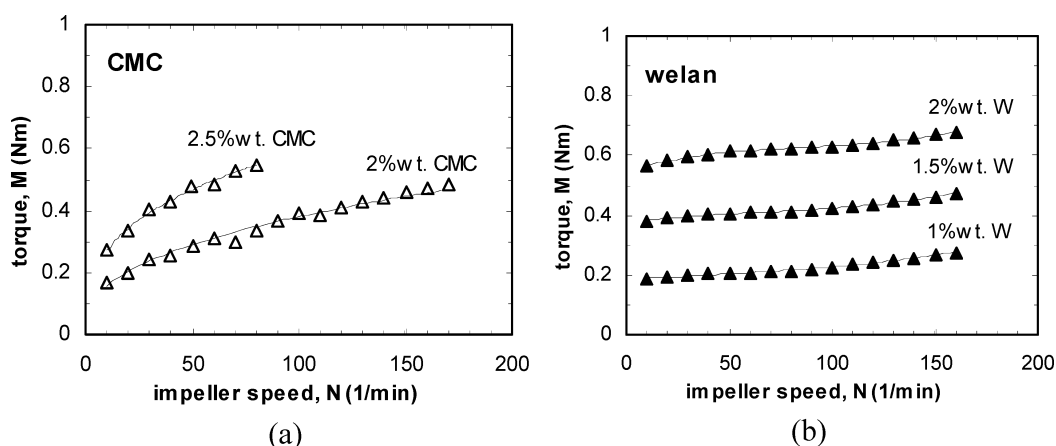


Fig. 5 – The dependence of torque,  $M$ , on impeller speed,  $N$ , for (a) CMC solutions and (b) welan solutions



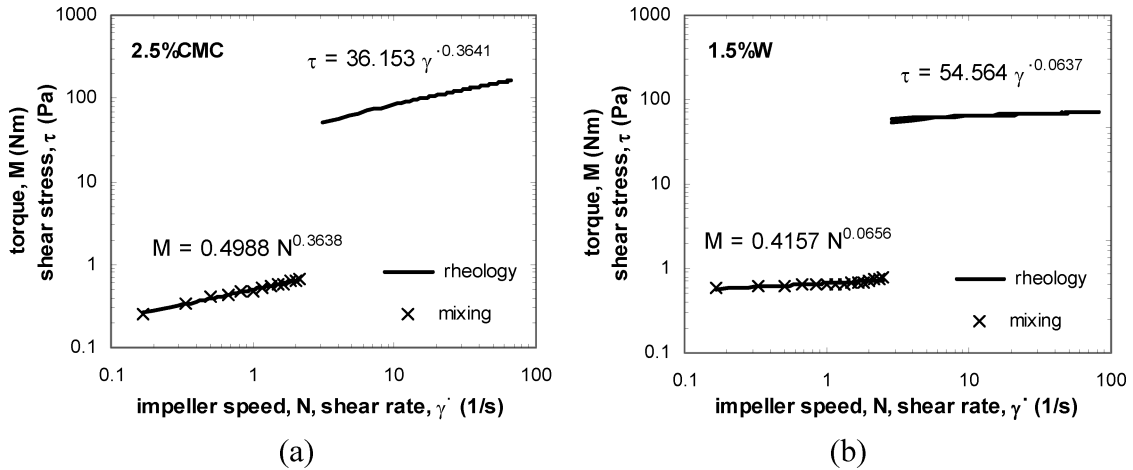


Fig. 7 – Comparison between rheological measurements and mixing experiments for a) 2.5 % wt. CMC and b) 1.5 % wt. W at  $T = 25\text{ }^{\circ}\text{C}$ : torque as a function of impeller speed and shear stress as a function of shear rate

tion (9), where the constants  $k$  and  $n$  were obtained from the dependence of shear stress on shear rate. In the mixing vessel, the shear dependent viscosity cannot be determined directly from the measurements of torque at different impeller speed. It can be calculated from equation (5), where the constant  $C$  is obtained from a set of experimental data for Newtonian fluid. As a result, the viscosity as a function of impeller speed can be obtained from measurements of torque at different impeller speeds. In the present work, the viscosity as a function of impeller speed was compared to the viscosity as a function of shear rate (obtained from rheological measurements). The results are presented in Fig. 8. The viscosity decreased with increasing impeller speed and shear rate, respectively, with the same slope, but the rheologically obtained curve was shifted. The value of the shift represented the constant  $K_s$  ( $\dot{\gamma} = K_s N$ ).

Constant  $K_s$  can be determined in different ways:

1. From a set of experimental data (equation (11)).
2. By shifting the viscosity curve from mixing experiments (viscosity vs. impeller speed):

$$\eta = k_2 N^{n-1} \tag{12}$$

towards rheologically obtained viscosity curve (viscosity vs. shear rate):

$$\eta = k_1 \dot{\gamma}^{n-1}. \tag{13}$$

By Metzner-Otto relation (equation (7))  $K_s$  can be obtained by combining equations (12) and (13):

$$K_s = \left( \frac{k_2}{k_1} \right)^{1/n-1} \tag{14}$$

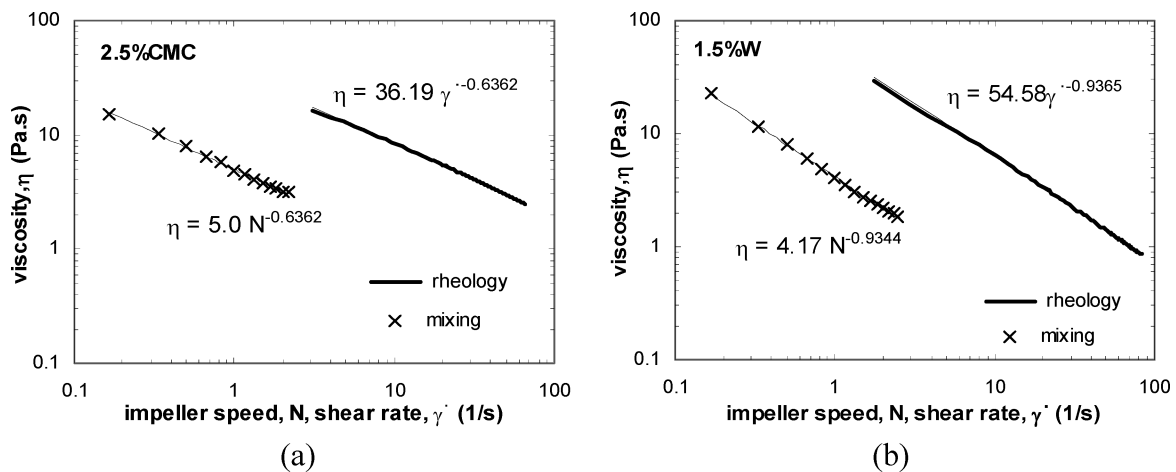


Fig. 8 – Comparison between rheological measurements and mixing experiments for a) 2.5 % wt. CMC and b) 1.5 % wt. W at  $T = 25\text{ }^{\circ}\text{C}$ : viscosity as a function of impeller speed and viscosity as a function of shear rate

3. By correlation. In the present work by a correlation, proposed by *Brito-De La Fuente* et al.<sup>10</sup>. The correlation was derived by following the extended Couette flow analogy:

$$K_s = 4\pi \frac{[(D_T/d_e)^2 - 1]^{1/(n-1)}}{\{n[(D_T/d_e)^{2/n} - 1]\}^{n/(n-1)}}, \quad (15)$$

where  $D_T$  is the diameter of the vessel,  $d_e$  the equivalent inside diameter, and  $n$  the power-law index. The quantity  $d_e$  depends solely on the geometry of the impeller (width of the impeller blade  $W$ , impeller diameter  $d$ ).<sup>10</sup>

$$\frac{d_e}{d} = \frac{D_T}{d} - 2 \frac{W}{d} \ln \left[ \frac{(D_T/d) - 1 + 2(W/d)}{(D_T/d) - 1} \right]. \quad (16)$$

The results of the two experimental and one theoretical determination of the constant  $K_s$  are presented in Table 3. For both CMC solutions, the experimentally obtained values of  $K_s$  were practically identical and in good agreement with the values obtained by the correlation. On the other hand, the experimental values of  $K_s$  for welan solutions were very close, but significantly lower from the values, obtained by a correlation, and lower than the values of CMC solutions. It can be concluded that the correlation, proposed by *Brito-De La Fuente* et al.<sup>10</sup> can be successfully used for power-law fluids with  $n > 0.1$  (CMC solutions), but not for  $n < 0.1$  (welan solutions). Furthermore,  $K_s$  depended on the type of the fluid.  $K_s$  increased with decreasing power-law index,  $n$ , or increasing CMC and welan concentration, respectively. This indicates that constant  $K_s$  depends not only on geometry of the impeller (which is reported in literature<sup>11</sup>), but also on rheological properties of the fluid (especially on the power-law index,  $n$ ).

Table 3 – Comparison of the values of  $K_s$  determined by correlation (equation (15)) and by experimental results

	n (/)	$K_s$ (/) correlation <sup>10</sup> equation 15	$K_s$ (/) experimental equation 14	$K_s$ (/) experimental equation 11
2 % wt. CMC	0.402	21.1	20.14	20.15
2.5 % wt. CMC	0.364	21.3	22.47	22.45
1 % wt. welan	0.081	23.45	15.28	15.28
1.5 % wt. welan	0.064	23.9	15.59	15.69
2 % wt. welan	0.05	24.3	15.64	15.73

The shear rate around the impeller in the mixing vessel was evaluated (equation (7)) by using the experimentally determined constant  $K_s$ . The viscosity as a function of shear rate in the mixing vessel was determined and compared to the rheologically obtained relation. Shear rate dependent viscosities are presented in Fig. 9; while consistency indices ( $k$ ) and flow behavior indices ( $n$ ) are presented in Table 4.

The comparison of different viscosity determinations (Fig. 9) showed, that the dependence of the viscosity on shear rate obtained by measuring the torque on the impeller closely followed the rheological measurements. For all the fluids studied, consistency indices ( $k$ ) and flow behavior indices ( $n$ ), obtained rheologically and by mixing experiments, showed very similar values. This means that for CMC and welan solutions studied the shear-dependent viscosity could be very precisely determined in mixing by measuring torque.

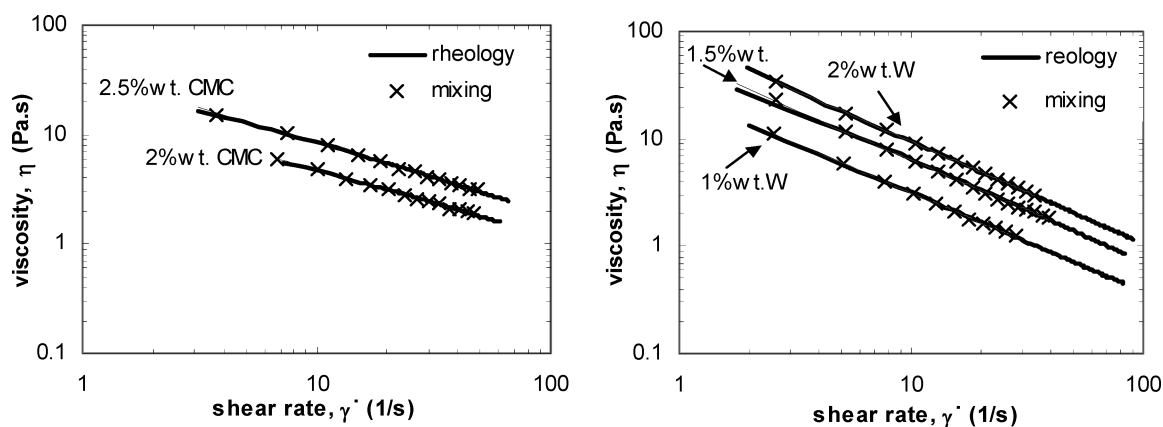


Fig. 9 – The dependence of viscosity on shear rate for CMC and welan solutions: comparison between the dependence obtained by rheological measurements (solid lines), and the dependence obtained by mixing experiments (symbols) – equation (5)

Table 4 – Comparison of constants  $k$  and  $n$  (equation (9)), obtained by rheological measurements and from mixing experiments

Fluid	$k$ (Pa.s <sup>n</sup> )		$n$ ( $l$ )	
	mixing	rheology	mixing	rheology
2 % wt. CMC	18.661	18.657	0.403	0.402
2.5 % wt. CMC	36.186	36.188	0.364	0.364
1 % wt. W	26.008	26.013	0.081	0.081
1.5 % wt. W	54.579	54.579	0.066	0.064
2 % wt. W	84.35	84.35	0.052	0.05

## Conclusions

The rheological characterization was performed in order to determine different rheological behavior of the fluids used. The results confirmed Newtonian behavior of, both, motor oils and shear-dependent non-Newtonian behavior of CMC and welan solutions, respectively. Under steady shear these fluids exhibited time-independent shear thinning flow behavior with different values of flow behavior indices ( $n$ ). Rheological tests under non-destructive shear conditions confirmed completely different rheological behavior of CMC and welan solutions. CMC solutions exhibited viscoelastic polymer solutions like properties, while welan properties were closer to weak gels. Due to complex rheological properties of welan solutions, significant discrepancies were obtained in mixing.

In the range of Reynolds number  $0.3 < Re < 40$  power curves (power number vs. Reynolds number) were determined by measuring torque at different impeller speeds. For all the fluids, the power number decreased with increasing Reynolds number with the slope of  $-1$ . The experimental points for oils and CMC solutions laid on the same line, while welan values were shifted toward higher values of  $C$ . The next difference was observed in value of shear rate constants  $K_s$ . Shear rate constants  $K_s$  were determined experimentally and calculated by a correlation. It was observed that experiments were in good agreement with the correlation for CMC solutions, but there were significant discrepancies for welan solutions. In the most of literature it is reported, that  $K_s$  depends only on the geometry of the impeller, whereas some of the authors<sup>10</sup> report on slight dependence of  $K_s$  on fluid properties. The results from our study showed that  $K_s$  is much more dependent on fluid properties. Experimentally determined shear rate constants  $K_s$  were used to calculate the dependence of the viscosity on shear rate in

the mixing vessel. Consistency indices ( $k$ ) and flow behavior indices ( $n$ ) were determined from mixing results. In all the fluids used, rheologically determined parameters were in good agreement with ones, obtained from mixing measurements. From these results, it can be concluded that the dependence of the viscosity on shear rate could be determined during mixing by measuring torque on the impeller. This is especially important for practical applications, where complex fluids like suspensions, fermentation broths, and other non-homogeneous fluids are used, and rheological determinations are often complex and unreliable.

## ACKNOWLEDGEMENT

This work was supported by the Slovenian Ministry of Education, Science and Sport through Grant P2-0191, Chemical Engineering.

## Nomenclature

$d$	– diameter of the impeller, m
$D_T$	– inside diameter of the vessel, m
$d_e$	– equivalent inside diameter, m
$h$	– ribbon height, m
$G'$	– elastic or storage modulus, Pa
$G''$	– viscous or loss modulus, Pa
$H$	– height of the fluid, m
$k$	– consistency index, Pa.s <sup>n</sup>
$K_S$	– shear rate constant
$M$	– torque, Nm
$N$	– impeller speed, s <sup>-1</sup>
$n$	– power-law index
$P$	– power input, W
$P_0$	– Power number
$Re$	– Reynolds number
$T$	– temperature, °C
$W$	– width of the impeller, m
$w$	– mass fraction

## Greek symbols

$\dot{\gamma}$	– shear rate, s <sup>-1</sup>
$\eta$	– viscosity, Pa s
$\rho$	– density, kg m <sup>-3</sup>
$\tau$	– shear stress, Pa

## Literature

1. Bakker, A., Gates, L. E., *Chem. Eng. Progress* (1995) 25-34.
2. Brito-De La Fuente, E., Choplin, L., Tanguy, P. A., *Trans IChemE* **69** (1991) 324.



3. *Takahashi, K., Yokota, T., Konno H.*, *J. Chem. Eng. Japan* **21** (1988) 63.
4. *Tanguy, P. A., Brito-de la Fuente, E.*, Non-newtonian mixing with helical ribbon impellers and planetary mixers, in *Siginer, D. A., De Kee, D., and Chhabra, R. P. (Ed.)*, *Advances in the flow and rheology of non-newtonian fluids, Part A*, pp. 301-330, Elsevier Science B. V., Netherlands, 1999.
5. *Brito-De La Fuente E., Choplin, L., Tanguy P. A.*, *Trans IChemE* **75** (1997) 45.
6. *Rielly, C. D.*, Mixing in food processing, in *Fryer, P. J., Pyle, D. L., and Rielly, C. D. (Ed.)*, *Chemical Engineering for the Food Industry*, Blackie Academic & Professional, London, 1997, pp. 383-433.
7. *Kemblowski, Z., Kristiansen, B.*, *Biotechnol. Bioeng.* **15** (1986) 1474.
8. *Barnes H. A.*, *A handbook of elementary rheology*, University of Wales, Aberystwyth, 2000.
9. *Metzner, A. B., Otto, R. E.*, *AIChE J.* **3** (1957) 3.
10. *Brito-de la Fuente, E., Leuliet, J. C., Choplin, L., Tanguy, P. A.*, *I. Chem. E. Symposium Series* **121** (1990) 75.
11. *Harnby, N., Edwards, M. F., Nienow, A. W.*, *Mixing in Process Industries*, Butterworth-Heinemann Ltd, Great Britain, 1992.

